Degradation Mechanisms and Early Detection of Moisture-Contaminated Lithium-ion Batteries

Shunling Li*
Amazon Innovation Center (Shenzhen) Co., Ltd.
Shenzhen, China
*shunlin@amazon.com

Zhigang Ai
Amazon Innovation Center (Shenzhen) Co., Ltd.,Shanghai Branch
Shanghai, China
aialbert@amazon.com

Xiaoman Li
Amazon Innovation Center (Shenzhen) Co., Ltd.,Shanghai Branch
Shanghai, China
uickili@amazon.com

***Abstract*—This study presents a systematic investigation of moisture-contaminated lithium-ion batteries through controlled perforations, combining performance analysis with an innovative early detection method. Performance testing revealed severe capacity degradation (<80% retention) and significant swelling (30-65%) in damaged batteries under both room-temperature cycling conditions and high-temperature/high-humidity storage (85°C/85% RH). Microscopic analysis uncovered the underlying mechanisms: moisture-induced Solid Electrolyte Interphase/Cathode Electrolyte Interphase (SEI/CEI) layer destruction and electrolyte decomposition, evidenced by structural deterioration and transition metal dissolution. Notably, our newly developed algorithm successfully identified compromised batteries at an early stage (>96% capacity retention) by analyzing capacity fade patterns, enabling preemptive intervention. Furthermore, Accelerating Rate Calorimetry (ARC) testing yielded unexpected results, with perforated batteries showing higher thermal runaway initiation temperatures (200±9°C vs 186±1.3°C) despite their compromised electrochemical performance. These findings advance both fundamental understanding of battery degradation and practical safety management strategies.**

Keywords—lithium-ion battery, moisture contamination, performance degradation, thermostability, early detection

I. Introduction

Lithium-ion batteries have become essential in various applications from consumer electronics to electric vehicles[1]. Their high energy density, long cycle life, and low self-discharge rate have made them the preferred choice for many applications. Polymer batteries are particularly notable for their lightweight and flexible characteristics[2].

However, safety and reliability concerns persist, especially regarding moisture exposure. Polymer batteries use thin aluminum-plastic laminate film packaging (typically 100-200 μm thick), which can be damaged during manufacturing, transportation, or usage[3]. Even minor punctures can compromise battery integrity, leading to moisture ingress and internal chemical reactions.

This study investigates these issues by creating five experimental groups (Group A-E) with precisely controlled package damage, featuring puncture diameters of 0.15, 0.20, 0.30, 0.40, and 0.50mm respectively. We conducted comprehensive analyses including high-temperature/high-humidity storage tests(85°C/85% relative humidity, abbreviated as HTHH), room-temperature cycling, and post-mortem examinations to track capacity retention, thickness expansion, and microstructural changes.

This study addresses two critical aspects: First, we investigate moisture-induced degradation mechanisms through systematic analysis of controlled package damage. Second, we develop an innovative algorithm for early detection of compromised batteries, identifying damage while capacity retention remains above 96%. Our thermal stability analysis also reveals unexpected characteristics of moisture-contaminated batteries, challenging conventional assumptions about moisture-induced safety risks[4].

II. Experimental

Commercial polymer lithium-ion batteries (5 Ah) with black aluminum-plastic laminate film packaging were used in this study. The batteries featured $LiCoO_2$ cathodes and graphite anodes, with $LiPF_6$ dissolved in ethylene carbonate/diethyl carbonate (EC/DEC) electrolyte. Controlled punctures (0.15-0.5mm) were created at the bottom corner of batteries using a precision milling machine equipped with metal needles of different diameters. The resulting perforations were examined using optical microscopy at 100× magnification, as shown in Fig. 1. Damaged batteries remained unsealed during testing to simulate real-world moisture ingress conditions.

Testing protocols included cycling performance evaluation at room temperature (25°C) using constant current protocols (3.5A for charging, 5A for discharging), combined with high-temperature/high-humidity (HTHH) storage at 85°C and 85% relative humidity with measurements taken at 6-hour intervals. Post-testing analysis consisted of battery disassembly at fully charged state in a controlled dry room environment, followed by detailed surface characterization using scanning electron microscopy (SEM) and compositional analysis via energy dispersive X-ray spectroscopy (EDS) to examine morphological changes and chemical composition of the electrodes. Accelerating rate calorimetry (ARC) was employed to assess thermal stability through analysis of self-heating initiation temperature (T_1) and thermal runaway initiation temperature (T_2), involving an initial controlled temperature ramp at 2° C per minute and switching to adiabatic mode upon detection of exothermic events. Additionally, an analytical algorithm was developed for early damage detection by monitoring capacity fade patterns, utilizing a detection threshold criterion of -0.0012

capacity fading gradient sustained over three consecutive measurement points to identify characteristic "dive points" indicating accelerated degradation.

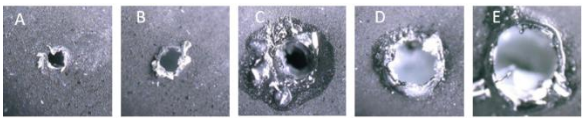

Fig. 1. Metal needles and optical microscope images (100×) of punctures with different diameters: (a) 0.15 mm, (b) 0.20 mm, (c) 0.30 mm, (d) 0.40 mm, and (e) 0.50 mm.

III. Results and Discussion

A. Cycling Performance

Room temperature cycling tests revealed stark performance differences between control and perforated batteries, as shown in Fig. 2. Control groups maintained excellent stability with approximately 95% capacity retention through 500 cycles, exhibiting minimal data scatter throughout the testing period. In contrast, perforated batteries demonstrated accelerated degradation with severity directly correlating to perforation size. Group E (0.5mm perforations) showed the most severe degradation, with capacity dropping below 80% within just 100 cycles. Groups with smaller perforations (0.15-0.3mm) performed better than those with larger perforations but still exhibited significant degradation compared to the control group. Notably, data variation increased with both perforation size and cycle number for damaged batteries, while remaining stable for control batteries, suggesting that moisture ingress leads to increasingly unpredictable degradation patterns over time.

Thickness measurements revealed even more dramatic differences, as illustrated in Fig. 3. Control batteries maintained remarkable stability with only approximately 5% swelling after 500 cycles and excellent consistency across samples. In stark contrast, larger perforations (0.4-0.5mm) led to severe thickness increases of 60-100% by cycle 200, while smaller perforations (0.15-0.3mm) showed more consistent but still significant swelling ranging from 30-50% increase. This severe swelling and capacity degradation can be attributed to multiple moisture-induced mechanisms: continuous destruction of the Solid Electrolyte Interphase (SEI) layer, electrolyte decomposition leading to gas evolution, loss of active lithium through side reactions, and progressive active material degradation. These results underscore that package integrity is crucial for long-term cycling stability, as even the smallest breach can lead to severe and unpredictable performance deterioration under normal operating conditions.

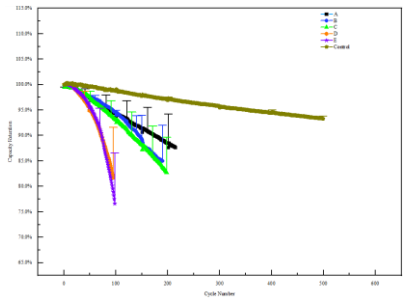

Fig. 2. Capacity retention versus cycle number for batteries at room temperature (25°C).

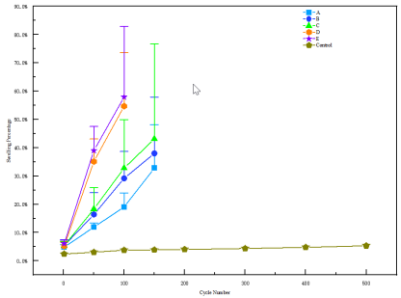

Fig. 3. Battery thickness changes versus cycle number at room temperature (25°C).

B. High Temperature and High Humidity Performance

Under 85°C/85% RH conditions over a 60-hour test period, intact control batteries demonstrated robust stability, maintaining approximately 95% capacity retention with swelling below 5%, as shown in Fig. 4 and Fig. 5. Perforated batteries, however, experienced rapid deterioration that intensified with perforation size—the 0.5mm group fell below 80% capacity between 42-48 hours of exposure, while smaller perforations (0.15-0.3mm) crossed this threshold near the 60-hour mark. Dimensional changes were even more pronounced, with larger holes (0.4-0.5mm) causing dramatic expansion of 40-65% within 60 hours and smaller perforations (0.15-0.3mm) resulting in 30-40% swelling. Performance variation among samples increased with both perforation size and exposure duration, indicating that moisture ingress under harsh environmental conditions leads to increasingly unpredictable degradation patterns. These accelerated degradation phenomena demonstrate that HTHH testing serves as an effective accelerated testing method, simulating the long-term effects of moisture contamination in a compressed timeframe. The results underscore the critical importance of package integrity for pouch batteries, as even minor breaches can trigger rapid and severe performance deterioration that far exceeds degradation rates observed under normal operating conditions.

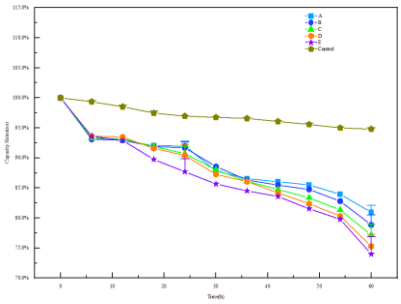

Fig. 4. Capacity retention versus storage time under high temperature (85°C) and humidity (85% RH) conditions.

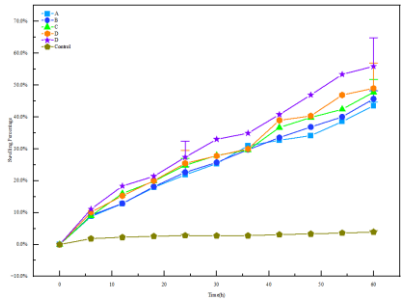

Fig. 5. Battery thickness changes versus storage time under high temperature (85°C) and humidity (85% RH) conditions.

C. *Surface Morphology Analysis*

The analysis of electrode surface morphology is crucial for understanding degradation mechanisms in lithium-ion batteries. In properly functioning cells, the graphite anode exhibits characteristic color changes corresponding to different lithiation states. As illustrated in Fig. 6, the anode color evolves systematically from black (pristine graphite) through various stages: greyish (LiC_{72} and LiC_{36} at 25% SOC), reddish-brown (LiC_{12} at 50% SOC), to golden-yellow (fully lithiated LiC_6 at 100% SOC)[5][6]. These color transitions serve as visual indicators of the lithiation degree and electrochemical functionality, providing a foundation for understanding moisture-induced degradation patterns.

Building on this understanding, we conducted comprehensive surface analysis using visual inspection, SEM, and EDS techniques to investigate moisture-induced degradation processes. These analyses revealed distinct patterns of deterioration in both cycled and HTHH-exposed samples.

The anode surface morphology revealed distinct degradation patterns under different conditions, as shown in Fig. 7. The pristine control sample (a) exhibited the characteristic golden color of fully lithiated graphite, indicating normal electrochemical functionality. After 60 hours of HTHH exposure, the control battery (b) maintained relatively good surface integrity, while the 0.5mm perforated sample (c) showed significant black and brown spots, indicating incomplete lithiation and surface degradation. The cycled samples showed similar trends - the normal battery after 120 cycles (d) retained good surface condition, whereas the 0.5mm perforated sample (e) displayed severe degradation with prominent black spots and visible lithium plating, particularly concentrated near the perforation site. This pattern suggests that moisture ingress accelerates electrolyte consumption, leading to local "dry-out" conditions that promote difficult lithiation and lithium plating. These observations align with our earlier capacity retention results, providing visual evidence of the accelerated degradation in perforated cells.

Fig. 6. Systematic observation of color transitions at six critical charging states (0-100% SOC)

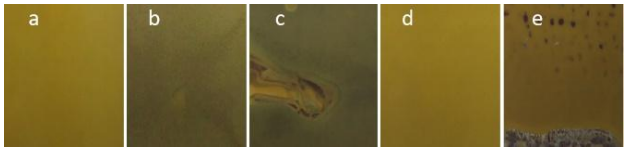

Fig. 7. Surface morphology of graphite anodes: (a) pristine, (b) control after 60h HTHH, (c) 0.5 mm perforated after 60h HTHH, (d) control after 120 cycles, (e) 0.5 mm perforated after 120 cycles.

SEM and EDS analyses (Fig. 8-9) revealed the detailed evolution of electrode surface morphology and composition. The pristine sample (a) displayed the characteristic graphite structure with well-defined particles, clear boundaries, and smooth surfaces typical of properly functioning anodes. Samples exposed to HTHH conditions or cycling without perforation (b and d) showed modest changes in surface morphology, with slight roughening of particle surfaces and minimal deposit formation. However, perforated samples (c and e) exhibited dramatic structural deterioration, characterized by severe disruption of the original graphite architecture, abundant irregular surface deposits, and the formation of numerous crystalline by-products scattered across the electrode surface. These crystalline formations, particularly prevalent in the perforated samples, indicate extensive electrolyte decomposition and secondary reaction products.

The degradation mechanism can be attributed to moisture-induced destruction of protective layers, which are Solid Electrolyte Interphase/Cathode Electrolyte Interphase(SEI/CET), triggering a series of parasitic reactions. The process begins with water molecules attacking the existing SEI components (primarily Li_2CO_3 and LiF), followed by hydrolysis of the electrolyte components[7][8][9].

$$LiPF_6 + H_2O \rightarrow LiF + 2HF + POF_3 \quad (1)$$

$$POF_3 + 3H_2O \rightarrow H_3PO_4 + 3HF \quad (2)$$

$$\langle EC|PC|DEC\rangle + H_2O \rightarrow ROH + CO_2 \quad (3)$$

(where R represents corresponding alcohol groups)These decomposition products further react to form various insoluble compounds:

$$Li^+ + F^- \rightarrow LiF \quad (4)$$

$$2Li^+ + {CO_3}^{2-} \rightarrow Li_2CO_3 \quad (5)$$

$$3Li^+ + {PO_4}^{3-} \rightarrow Li_3PO_4 \quad (6)$$

EDS analysis provided quantitative evidence of these degradation processes, showing elevated levels of F and P elements in degraded regions. The detection of Co signals further indicated cathode dissolution and subsequent deposition on the anode surface. These findings, combined with the schematic illustration in Fig. 10, demonstrate how moisture ingress initiates a cascade of detrimental reactions, ultimately leading to the observed capacity fade and swelling behaviors.

The comprehensive surface analysis confirms that moisture contamination triggers multiple degradation pathways, including SEI/CEI destruction, electrolyte decomposition, and transition metal dissolution, collectively contributing to the severe performance deterioration observed in perforated batteries[10]. Having established the structural and chemical changes caused by moisture ingress, we next investigated its impact on battery thermal stability.

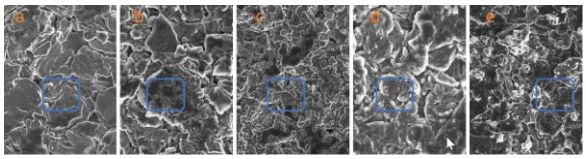

Fig. 8. SEM micrographs of anode surfaces: (a) pristine, (b) control after HTHH, (c) 0.5 mm perforated after HTHH, (d) control after 120 cycles, (e) 0.5 mm perforated after 120 cycles.

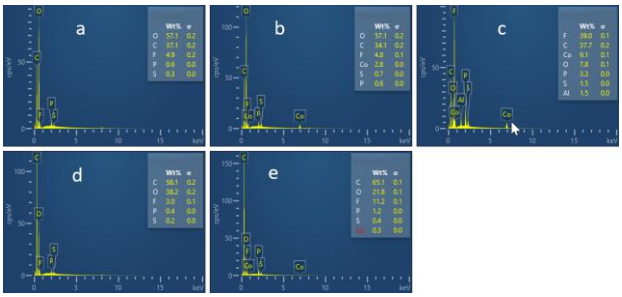

Fig. 9. EDS spectra from regions marked in Fig. 7.

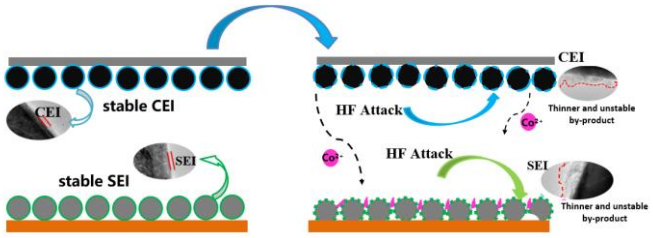

Fig. 10. Schematic Illustration of HF-Induced Degradation Mechanism on SEI and CEI Protective Layers in Lithium-ion Batteries

D. *Thermostability Performance*

Thermal stability characteristics of cycled batteries were evaluated using ARC testing, focusing on self-heating initiation temperature (T_1) and thermal runaway initiation temperature (T_2). Tests were conducted on both perforated (0.5mm hole) and control batteries after 120 cycles, when their capacity retentions were approximately 80% and 98% respectively.

The ARC results revealed that perforated batteries consistently exhibited lower self-heating initiation temperatures, with average T_1 values of 60±7.5°C compared to 75±2.8°C for control samples, as shown in Fig. 11. This approximately 15°C reduction in T_1 can be attributed to the presence of lithium plating in moisture-compromised batteries, as confirmed by our previous SEM observations. Notably, the larger standard deviation in perforated samples reflects the non-uniform degradation patterns caused by moisture ingress.

Perforated batteries showed higher thermal runaway initiation temperatures (200±9°C) compared to the more consistent control samples (186±1.3°C). This enhanced yet more variable thermal stability likely results from three factors: improved heat dissipation through the perforation, reduced electrolyte content due to moisture-induced decomposition, and lower overall energy content from capacity fade[11][12].

These findings challenge conventional assumptions about moisture contamination and battery safety. Despite significant electrochemical performance degradation, perforated batteries maintained, and in some aspects improved, thermal stability compared to intact batteries. The comprehensive ARC results indicate that while moisture ingress severely impacts battery performance, it does not necessarily compromise thermal safety characteristics.

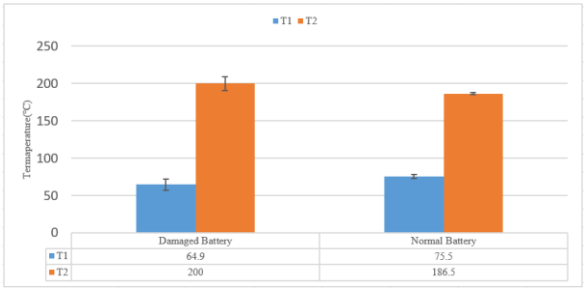

Fig. 11. Thermal parameters of normal and perforated (0.5 mm) batteries after 120 cycles. T_1: self-heating initiation temperature, T_2: thermal runaway initiation temperature.

E. *Battery Damage Detection Algorithm*

Based on the distinct degradation patterns observed in our performance studies, we developed an innovative approach for early identification of damaged batteries. As illustrated in Fig. 12, the algorithm successfully detected a 'dive point' for damaged batteries (0.5mm perforation) at cycle 48, where the capacity retention was still maintaining 98.6%. This early detection was achieved by monitoring the capacity fade rate, with our criterion set at a gradient threshold of -0.0012 persisting for three consecutive data points. The figure demonstrates both the capacity retention curve and the corresponding gradient analysis, clearly showing the characteristic acceleration point where degradation transitions from normal to abnormal patterns. In contrast, Fig. 13 shows a typical normal battery where no such dive point could be identified using the same criteria, indicating stable degradation behavior throughout the cycling process.

Analysis of multiple damaged batteries revealed dive points occurring between 49-76 cycles, all with capacity retentions above 96%. Normal batteries showed no such dive points throughout the cycling process. The mean gradient of capacity fade for damaged batteries ranged from -0.001488 to -0.002992, significantly higher than that of normal batteries (-0.000094 to -0.000158). This substantial difference in degradation rates provides a robust basis for distinguishing compromised batteries from healthy ones at an early stage.

By implementing this algorithm in battery management systems, it becomes possible to identify compromised batteries at an early stage. Although our ARC results show that damaged batteries maintain comparable thermal stability to normal ones, the risk of electrolyte leakage and other potential hazards associated with package damage necessitates early detection and intervention. This early warning system enables timely identification of at-risk batteries, allowing for preventive measures before any adverse incidents occur. This algorithm also can identify batteries experiencing rapid degradation due to other factors, offering a practical method for real-time monitoring and enhancing the overall safety of lithium-ion battery applications.

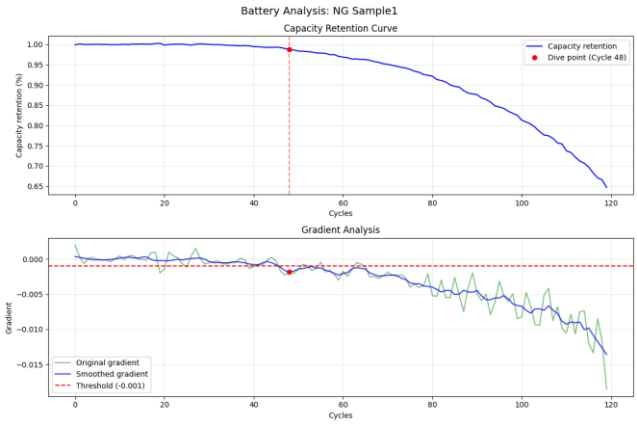

Fig. 12. Early detection of capacity fade acceleration in damaged battery: Identification of dive point at cycle 48 with 98.6% capacity retention using gradient threshold criterion (-0.0012 for three consecutive points).

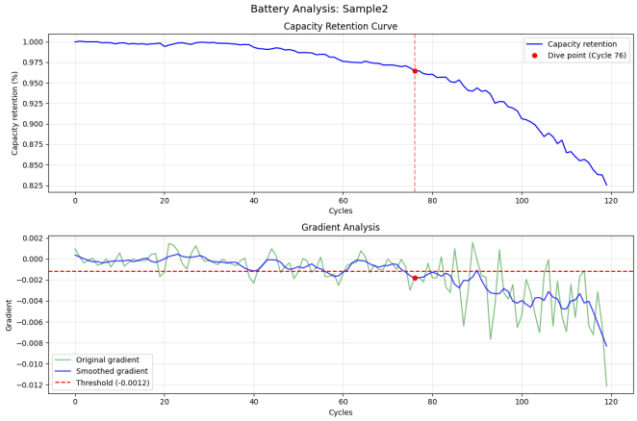

Fig. 13. Capacity retention curve of normal battery showing no dive point detection under the same gradient threshold criterion.

IV. Conclusion

This comprehensive study has yielded four key findings that significantly advance battery safety management. First, systematic analysis established clear correlations between package damage and degradation severity - even minimal perforation (0.15mm) triggered severe capacity fading and swelling, with larger damage accelerating degradation below 80% capacity within 100 cycles or 48 hours under HTHH conditions.

Second, microscopic and spectroscopic analyses provided direct evidence of degradation mechanisms through SEI/CEI destruction, electrolyte decomposition, and transition metal dissolution. Third, thermal stability evaluation challenged conventional assumptions - perforated batteries exhibited enhanced thermal runaway resistance (200±9°C vs 186±1.3°C) despite compromised electrochemical performance.

Most significantly, we developed and validated an algorithm capable of detecting battery damage while capacity retention remains above 96%. These findings address both fundamental and practical aspects of battery safety, offering valuable guidance for quality control protocols and safety management strategies in industrial applications.

References

[1] B. K. Park, Y. K. Jeong, S. Y. Yang, et al., "Deterioration behavior of aluminum pouch film used as packaging materials for pouch-type lithium-ion batteries," Journal of Power Sources, vol. 483, pp. 230222, Jan. 2021.

[2] T. Zhang, "Performance degradation and sealing failure analysis of pouch lithium-ion batteries under multi-storage conditions," Journal of Power Sources, vol. 571, pp. 232710, Mar. 2024.

[3] D. Ouyang, M. Chen, J. Weng, et al., "Exploring the thermal stability of lithium-ion cells via accelerating rate calorimetry: A review," Journal of Energy Chemistry, vol. 81, pp. 543-573, Apr. 2023.

[4] F. Grimsmann, T. Gerbert, F. Brauchle, et al., "Hysteresis and current dependence of the graphite anode color in a lithium-ion cell and analysis of lithium plating at the cell edge," Journal of Energy Storage, vol. 15, pp. 17-22, Feb. 2018.

[5] T. Hoidene, M. Monchak, V. Baran, A. Khele, M. J. Munhbauer, V. Dyadkin, A. Rabenbauer, A. Schökel, H. Ehrenberg, P. Müller-Buschbaum, A. Senyshyn, "Thermal structural behavior of electrochemically lithiated graphite (LixC6) anodes in Li-ion batteries," Batteries & Supercaps, vol. 1, no. 1, pp. 1-14, Jan. 2024.

[6] P. U. Nzereoguo, A. D. Omah, F. I. Ezema, E. I. Iwuoha, A. C. Nwanya, "Anode materials for lithium-ion batteries: A review," Applied Surface Science Advances, vol. 9, pp. 100233, Jun. 2022.

[7] H. Adenusi, G. A. Chass, S. Passerini, et al., "Lithium batteries and the solid electrolyte interphase (SEI)—Progress and outlook," Advanced Energy Materials, vol. 13, pp. 2203307, Mar. 2023.

[8] A. Wang, S. Kadam, H. Li, et al., "Review on modeling of the anode solid electrolyte interphase (SEI) for lithium-ion batteries," npj Computational Materials, vol. 4, pp. 15, Feb. 2018.

[9] S. J. An, J. Li, C. Daniel, et al., "The state of understanding of the lithium-ion-battery graphite solid electrolyte interphase (SEI) and its relationship to formation cycling," Carbon, vol. 105, pp. 52-76, Aug. 2016.

[10] J. L. Tebbe, A. M. Holder, C. B. Musgrave, "Mechanisms of LiCoO2 cathode degradation by reaction with HF and protection by thin oxide coatings," ACS Applied Materials & Interfaces, vol. 7, no. 43, pp. 24265-24278, Oct. 2015.

[11] J. Lamb, L. Torres-Castro, J. C. Hewson, R. C. Shurtz, Y. Preger, "Investigating the role of energy density in thermal runaway of lithium-ion batteries with accelerating rate calorimetry," Journal of The Electrochemical Society, vol. 168, no. 6, pp. 060516, Jun. 2021.

[12] Y. Yue, Z. Jia, Y. Li, Y. Wen, Q. Lei, Q. Duan, J. Sun, Q. Wang, "Thermal runaway hazards comparison between sodium-ion and lithium-ion batteries using accelerating rate calorimetry," Process Safety and Environmental Protection, vol. 189, pp. 61-70, Sept. 2024.